The Glycine[1] Residue in Cyclic Lactam Analogues of Galanin(1−16)-NH_2 Is Important for Stabilizing an N-Terminal Helix

Katharine A. Carpenter,* Ralf Schmidt, Shi Yi Yue, Lejla Hodzic, Chantevy Pou, Kemal Payza, Claude Godbout, William Brown, and Edward Roberts

AstraZeneca R&D Montréal, 7171 Frédérick-Banting, Saint-Laurent, Québec, Canada H4S 1Z9

Received May 12, 1999; Revised Manuscript Received August 26, 1999

ABSTRACT: The neuropeptide galanin is a 29- or 30-residue peptide whose physiological functions are mediated by G-protein-coupled receptors. Galanin's agonist activity has been shown to be associated with the N-terminal sequence, galanin(1−16). Conformational investigations previously carried out on full-length galanin have, furthermore, indicated the presence of a helical conformation in the neuropeptide's N-terminal domain. Several cyclic lactam analogues of galanin(1−16)-NH_2 were prepared in an attempt to stabilize an N-terminal helix in the peptide. Here we describe and compare the solution conformational properties of these analogues in the presence of SDS micelles as determined by NMR, CD, and fluorescence spectroscopy. Differences in CD spectral profiles were observed among the compounds that were studied. Both c[D^4,K^8]Gal(1−16)-NH_2 and c[D^4,K^8]Gal(1−12)-NH_2 adopted stable helical conformations in the micelle solution. On the basis of the analyses of their respective αH chemical shifts and NOE patterns, this helix was localized to the first 10 residues. The distance between the aromatic rings of Trp^2 and Tyr^9 in c[D^4,K^8]Gal(1−16)-NH_2 was determined to be 10.8 ± 3 Å from fluorescence resonance energy transfer measurements. This interchromophore spacing was found to be more consistent with a helical structure than an extended one. Removal of the Gly^1 residue in compounds c[D^4,K^8]Gal(1−16)-NH_2 and c[D^4,K^8]-Gal(1−12)-NH_2 resulted in a loss of helical conformation and a concomitant reduction in binding potency at the GalR1 receptor but not at the GalR2 receptor. The nuclear Overhauser enhancements obtained for the Gly^1 deficient analogues did, however, reveal the presence of nascent helical structures within the N-terminal sequence. Decreasing the ring structure size in c[D^4,K^8]Gal(1−16)-NH_2 by replacing Lys^8 with an ornithine residue or by changing the position of the single lysine residue from eight to seven was accompanied by a complete loss of helical structure and dramatically reduced receptor affinity. It is concluded from the data obtained for the series of cyclic galanin(1−16)-NH_2 analogues that both the ring structure size and the presence of an N-terminal glycine residue are important for stablilizing an N-terminal helix in these compounds. However, although an N-terminal helix constitutes a predominant portion of the conformational ensemble for compounds c[D^4,K^8]Gal(1−16)-NH_2 and c[D^4,K^8]Gal(1−12)-NH_2, these peptides nevertheless are able to adopt other conformations in solution. Consequently, the correlation between the ability of the cyclic galanin analogues to adopt an N-terminal helix and bind to the GalR1 receptor may be considered as a working hypothesis.

Galanin is a 29- or 30-amino acid linear neuropeptide that is found throughout the central and peripheral nervous systems as well as the gastrointestinal tract of several mammalian species (*1*−*4*). It is a potent inhibitor of insulin release (*5*, *6*) and a stimulator of growth hormone release (*7*) and has been shown to inhibit acetylcholine release in the hippocampus (*8*). The neuropeptide is also known to stimulate feeding behavior in rats when injected into the hypothalamus (*9*) and is believed to have a tonic role in the control of pain threshold (*10*). Identification of the amino acid sequences for galanin isolated from several species has indicated an absolute conservation within the first 15 residues (*2*, *4*).

The actions of galanin are mediated through its interaction with distinct G-protein-coupled receptor subtypes, three of which have been cloned and termed GalR1,[1] GalR2, and GalR3 (*11*−*15*). Results from hydropathy analyses have suggested that all three receptors belong to the seven-transmembrane G-protein-coupled receptor superfamily. Expression of the GalR1 receptor is known to be restricted

* To whom correspondence and reprint requests should be addressed: AstraZeneca R&D Montréal, 7171 Frédérick-Banting, Saint-Laurent, Québec, Canada H4S 1Z9. Telephone: (514) 832-3200. Fax: (514) 832-3232. E-mail: katharine.carpenter@astrazeneca.com.

[1] Abbreviations: NMR, nuclear magnetic resonance; CD, circular dichroism; NOESY, nuclear Overhauser enhancement spectroscopy; TOCSY, total correlation spectroscopy; TSP, 3,3,3-trimethylsilylpropionate; SDS, sodium dodecyl sulfate; FRET, fluorescence resonance energy transfer; NOE, nuclear Overhauser enhancement; Orn, ornithine; HPLC, high-performance liquid chromatography; EDTA, ethylenediaminetetraacetic acid; BSA, bovine serum albumin; TB, level of total binding; NS, level of nonspecific binding; SB, level of specific binding; FBS, fetal bovine serum; GDP, guanosine diphosphate; CON, mean level of control binding; STM, mean level of stimulated binding; hgal, human galanin; hGalR1, human GalR1 receptor; rGalR2, rat GalR2 receptor; dpm, disintegrations per minute.

10.1021/bi991081i CCC: $18.00
Published on Web 10/23/1999

Table 1: Structures of Galanin Analogues

Peptide	*1*	*5*	*10*	*15*
1. galanin(1-16)-NH_2	G W T L N S A G Y L L G P H A V -NH_2			
2. c[D^4,K^8]gal(1-16)-NH_2	G W T[D N S A K]Y L L G P H A V -NH_2			
3. c[D^4,K^8]gal(2-16)-NH_2	W T[D N S A K]Y L L G P H A V -NH_2			
4. c[D^4,K^8]gal(1-12)-NH_2	G W T[D N S A K]Y L L G -NH_2			
5. c[D^4,K^8]gal(2-12)-NH_2	W T[D N S A K]Y L L G -NH_2			
6. c[D^4,K^7]gal(1-16)-NH_2	G W T[D N S K]G Y L L G P H A V -NH_2			
7. c[D^4,Orn^8]gal(1-16)-NH_2	G W T[D N S A Orn]Y L L G P H A V -NH_2			

to the brain and spinal cord (*12*, *15*), whereas GalR3 has been detected in the peripheral tissues only (*14*). The GalR2 receptor is more widely distributed within the central and peripheral nervous systems (*13*, *16*).

Studies involving L-Ala-substituted analogues of galanin have identified Trp^2, Asn^5, and Tyr^9 as well as the N-terminal amino group as being critical determinants for GalR1 receptor binding (*17*, *18*). N-Terminal fragments of galanin are, furthermore, capable of eliciting a full agonist response at the hippocampal and hypothalamic galanin receptors (*17*, *19*). Among the C-terminally truncated galanin analogues that have been studied, Gal(1−13)-NH_2 is the shortest peptide that is able to bind with nanomolar binding affinity to the hypothalamic galanin receptor (*17*). It has also been demonstrated that removal of the N-terminal glycine in galanin results in an analogue which is considerably more selective for the GalR2 receptor (*13*).

Conformational investigations of galanin have been carried out under a variety of solution conditions (*20*−*24*). Experimental and computational techniques employed for these studies have included CD spectroscopy, NMR spectroscopy, IR spectroscopy, and molecular dynamics simulations. In purely aqueous solution, galanin was found to exhibit a primarily disordered conformation (*20*). Evidence for the presence of a nascent helix encompassing residues 3−11 was, however, obtained from an NMR spectroscopic analysis of the full-length peptide in water (*21*). When dissolved in 2,2,2-trifluoroethanol, galanin adopted a conformation consisting of two helices interrupted by a bend at Pro^{13} (*22*). Helical structures in galanin and its N-terminal fragments Gal(1−16) and Gal(1−12) were also found to be stabilized in the presence of negatively charged lipid vesicles (*23*). In a recent article, the NMR-derived conformation of porcine galanin in an SDS micelle solution was described (*24*). The reported conformation contained well-defined β and γ turns in the regions Gly^1−Asn^5, Ala^7−Leu^{10}, and Asp^{24}−Gly^{27} but was otherwise disordered.

Peptides chosen for conformational analysis in this study include analogues of Gal(1−16)-NH_2 and Gal(2−16)-NH_2 incorporating a (i,i+4) or (i,i+3) side chain to side chain cyclization via lactam bridge formation (peptides **2**−**7**; Table 1). Inclusion of a lactam bridge in the peptides was done in an attempt to promote stabilization of a helical structure in the N-terminal region of the galanin analogues. The rational for carrying out structure activity studies on helical galanin analogues is based on a recently published model describing the binding of galanin to its GalR1 receptor (*25*). In this model, critical residues in the neuropeptide interacted optimally with proposed binding site residues in the receptor when galanin contained an N-terminal helical conformation.

In an effort to examine the relevance of helicity in galanin for receptor binding and possibly receptor selectivity, conformational studies have been carried out on the cyclic galanin analogues presented in Table 1 using CD spectroscopy, NMR spectroscopy, and fluorescence resonance energy transfer (FRET) techniques. Negatively charged SDS micelles were included in the peptide aqueous samples due to their known ability to promote secondary structures in galanin analogues and to provide a membrane mimetic environment (*26*). Results from the spectroscopic analyses presented in this paper indicate that a two-turn helical structure extending to the N-terminus of galanin may be important for galanin receptor binding.

MATERIALS AND METHODS

Materials. Peptide synthesis was performed on an Avanced ChemTech MOS 496 multiple-peptide synthesizer using Fmoc-Rink-Amide-MBHA resin (Novabiochem, substitution of 0.6 mmol/g of resin) as the starting material. Standard coupling protocols were employed for these syntheses. For the cyclic analogues, N-terminally Fmoc-protected cyclization precursors were first cleaved from their resin. Cyclization of these peptides to their final products then proceeded in solution using PyBOP as the coupling reagent. In general, the cyclic products were obtained in high yield. The peptides were established to be at least 98% pure by reversed phase HPLC in two different solvent systems. A correct molecular weight was obtained for each peptide via electrospray mass spectrometry. Amino acid compositions of the peptides were confirmed by amino acid analysis.

Iodinated human galanin ([^{125}I]hGal) was either obtained from Amersham (catalog no. NEX333) or prepared in house. The in-house preparation method involved chloramine T iodination of the human galanin peptide previously obtained from Bachem (H-8230). The monoiodinated product was purified to homogeneity (2200 Ci/mmol) by reverse-phase HPLC. The source of radioiodine was Na^{125}I (catalog no. NEZ-033H from Dupont/NEN, Boston, MA). The other radioligand that was used, guanosine 5′-*O*-(3-[^{35}S]thio)-triphosphate GTPγ[^{35}S], 1000 Ci/mmol, cataolg no. NEG-030H), was from Dupont/NEN. Sodium dodecyl-d_{25} sulfate (SDS-d_{25}) and deuterium oxide were purchased from CDN Isotopes (Montreal, PQ). Nondeuterated SDS was obtained from Bio-Rad.

Cell Culture and Membrane Preparation for Receptor Binding and GTPγ[^{35}S] Binding Assays. The rGalR2 membranes were prepared from human HEK-293S cells expressing the cloned rat GalR2 receptor and Geneticin resistance. The hGalR1 membranes were from human Bowes melanoma cells originally obtained from ATCC (Rockville, MD). Both types of cells were grown in suspension at 37 °C in 5% CO_2 in a 20 L bioreactor with a helicoidal ribbon impeller containing calcium-free DMEM (Bio Whittaker, Inc., Walkersville, MD), 5% iron-enriched bovine calf serum (Intergen, Purchase, NY), and 0.1% Pluronic F-68 (Gibco BRL, Burlington, ON). Cells were harvested from culture, pelleted, and resuspended in ice-cold lysis buffer [50 mM Tris (pH 7.0) and 2.5 mM EDTA]. Phenylmethanesulfonyl fluoride was added just prior to use to a concentration of 0.1 mM (from a 0.1 M stock in ethanol). After lysis on ice for 15 min, the cells were gently homogenized for 30 s with a

polytron. The suspension was spun at 1000*g* (maximum) for 10 min at 4 °C. The supernatant was saved on ice, and the pellets were resuspended gently and spun as described before. The supernatants from both spins were combined and spun at 46000*g* (maximum) for 30 min. The pellets were carefully resuspended in cold Tris buffer [50 mM Tris-HCl (pH 7.0)] and spun again. The final pellets were resuspended gently in membrane buffer [50 mM Tris and 0.32 M sucrose (pH 7.0)]. Aliquots (1 mL) in polypropylene tubes were frozen in dry ice/ethanol and stored at −70 °C until they were used. The protein concentration was determined using BSA as a standard in a modified Lowry assay with sodium dodecyl sulfate.

Receptor Binding Assays. The ability of test compounds to compete with trace radioligands for binding to each receptor type was assessed. In these experiments, a test compound together with radioactive galanin was allowed to reach binding equilibrium with membranes from cells expressing one of the galanin receptors. The affinities of test compounds for the receptor subtypes were then determined from their resultant competitive displacement curves. The experimental protocol consisted of the following steps. Membranes were thawed at 37 °C, cooled to 4 °C, passed three times through a 25-gauge needle, and diluted into 50 mM Tris, 3 mM $MgCl_2$, 2.5 mg/mL BSA, and 3.75 μM β-endorphin (pH 7.4). Aliquots (80 μL) of membranes were added to 96-well plates containing about 55 000 dpm (0.037 nM) of the radioligand (70 μL) and test compounds (150 μL) at various concentrations in a total volume of 300 μL. The final concentration of β-endorphin was thus 1 μM. Compounds were tested either in a range spanning five dilutions, 10-fold apart, or in a range spanning 10 dilutions, 2.5-fold apart. The levels of total (TB) and nonspecific (NS) binding were determined in the absence and presence of 100 nM hGal, respectively. The contents of the plates were mixed and the plates incubated at 25 °C for 90 min, after which time the contents were rapidly vacuum-filtered through Packard GB/B Unifilter plates which had been presoaked for at least 2 h in 0.1% polyethyleneimine. The filters were subjected to three rapid washes (1 mL each) of wash buffer [50 mM Tris (pH 7.0) and 3 mM $MgCl_2$]. The Unifilter plates were dried in an oven at 55 °C for 2 h. The plates were then counted in the 2.9−100 keV window in a TopCount instrument (Packard) following addition of 50 μL of MS-20 scintillation fluid per well. For each 96-well plate, eight wells were used to define mean TB and eight to define mean NS. The level of control specific binding (SB) was calculated as TB minus NS. The SB in the presence of test compound was determined as the mean of duplicate TB minus mean NS measurements. The SB at each concentration of test compound was then expressed as a percentage of control SB. Outlying points that differed by >20% from the duplicate determination were not used. IC_{50} values for ligands displacing specifically bound radioligand were obtained from sigmoidal fits of their respective curves using a nonlinear curve-fitting program (Prism version 2.01 from GraphPad Software, San Diego, CA).

GTPγ[^{35}S] Binding Assay. For the GTP binding assay, GTPγ[^{35}S] was combined with test compounds and membranes from human Bowes melanoma cells which express GalR1 receptors. The experiments were designed to measure the abilities of compounds to stimulate the binding of GTPγ[^{35}S]to G-proteins coupled to GalR1 receptors. Human galanin (hGal, 1 μM) elicited about 2-fold stimulation of GTPγ[^{35}S] binding to membranes of Bowes cells. The maximal effect (E_{max}) of hGal was used to define a reference point of 100%. The assay was adapted from published procedures (*27*, *28*). Membranes were thawed at 37 °C, cooled on ice, passed three times through a 25-gauge needle, and diluted to a concentration of 187.5 μg/mL in GTP assay buffer [50 mM Hepes, 20 mM NaOH, 5 mM $MgCl_2$, 100 mM NaCl, 1 mM EDTA, 0.1% BSA, and 15 μM guanosine diphosphate (GDP) (pH 7.4)]. The components were added in the following order to 96-well microtiter plates: 150 μL of test substance, 80 μL of membrane preparation (15 μg of protein), and then, after preincubation for 15 min, 70 μL of GTPγ[^{35}S] (~170000 dpm). Eight wells per plate contained 150 μL of buffer to define control binding. Human galanin (1 μM) was included in eight other wells to define the maximal level of stimulated binding. The plates were vortexed, incubated for 45−60 min at 25 °C, and then filtered over GF/B filters (or Packard GF/B Unifilter plates) presoaked for 1 h in water. Unifilters were washed with 3 × 1 mL of ice-cold wash buffer [50 mM Tris, 5 mM $MgCl_2$, and 50 mM NaCl (pH 7)]. The Unifilter plates were dried in an oven at 55 °C for 2 h, and then counted in the ^{14}C window in a TopCount instrument (Packard) after adding 50 μL of MS-20 scintillation fluid/well. The disintegrations per minute values of the control wells were averaged to define the mean level of control binding (CON). Those containing 1 μM hGal were averaged to define the mean level of stimulated binding (STM). The disintegrations per minute values of GTPγ[^{35}S] binding obtained in the presence of test compound (DPM) were converted to percent stimulated binding with the equation 100 × (DPM − CON)/(STM − CON). Values of EC_{50} and E_{max} for ligands in stimulating [γ-^{35}S]GTP binding were obtained from sigmoidal fits of a nonlinear curve-fitting program (Prism version 1.0, 2.0, or 2.01 from GraphPad Software). Outlying points, which deviated from the corresponding duplicate determination by more than 10%, were not used in the calculations.

Measurement of the Level of Intracellular Calcium Using the FLIPR System. HEK-293S cells (clone 44) expressing the rat galanin subtype 2 receptor were obtained by stable transfection. Cells were grown as monolayers in Falcon flasks using Dulbecco's modified Eagle's medium (DMEM) containing high glucose and L-glutamine (2 mM), 10% fetal bovine serum (FBS), penicillin (100 units/mL), streptomycin (100 μg/mL), fungizone (0.25 μg/mL), and G-418 (Geneticin, 600 μg/mL). Drugs were prepared in Hank's BSS (without phenol red), 20 mM HEPES, and 0.1% BSA (pH 7.4) (200 μL per well, 3 times the final concentration) in 96-well clear v-bottom plates (Sarstedt, catalog no. 82.1583). This procedure was carried out on the day of the experiment or the previous day. The plates were kept at 4 °C overnight and removed 2 h prior to experimentation. Cells (10−12 million) were resuspended to a single cell solution, counted, centrifuged, and resuspended in 10 mL of loading medium containing 4 μM Fluo-3, AM (Molecular Probes, catalog no. F-1241), and 0.02% pluronic acid (Molecular Probes, catalog no. P-6867). The cells were incubated in a sterile flask for 1 h in an incubator at 37 °C in 5% CO_2. Following the incubation step, cells were washed four times in 30 mL of Hank's BSS, 20 mM Hepes, and 0.1% BSA (pH 7.4) and

resuspended in wash buffer. The cells were plated in clear, flat-bottom, poly-D-lysine-coated black 96-well plates (VWR, catalog no. 356640) at a density of 100 000 per well per 100 μL and spun at 200*g* for 3 min at room temperature. The assay was conducted on the FLIPR system (argon laser at 488 nm; exposure time set to 0.4 s) to assess the mobilization of intracellular calcium in response to 50 μL applications of different drugs. The data were analyzed in sigmoidal fits using GraphPad Prism to obtain the maximum level of activation (%E_{max} of rat galanin) and EC_{50} values.

Sample Preparation. NMR samples of peptides **2**−**7** shown in Table 1 were prepared by dissolving 1.0−1.4 mg of peptide and 31 mg of SDS-d_{25} in 500 μL of 50 mM sodium phosphate buffer (90% H_2O/10% D_2O, pH 6.2). The final peptide and SDS-d_{25} concentrations were 1.5 and 200 mM, respectively. Since aggregation was first apparent upon the preparation of a 1.5 mM sample of c[D^4,K^8]Gal(2−16)-NH_2, it was necessary to lower the peptide sample concentration to 0.75 mM in this case. The pH measured for each sample was 6.2, and samples were used without further pH adjustment.

Each sample examined by CD spectroscopy consisted of 1−1.5 mg of peptide and 29 mg of SDS dissolved in 500 μL of 50 mM sodium phosphate buffer (pH 6.2). The final peptide concentration was 1.5 mM, and the sample pH was 6.2. Diluted samples of the cyclic peptides shown in Table 1 were prepared by pipetting 100, 100, and 25 μL aliquots of each 1.5 mM parent solution into three separate vials. To the three vials for each compound were then added respectively, 100, 300, and 475 μL volumes of an SDS stock solution [200 mM SDS in 50 mM sodium phosphate buffer (pH 6.2)]. This resulted in the formation of solutions with peptide concentrations of 0.75, 0.38, and 0.075 mM.

For the fluorescence resonance energy transfer (FRET) experiments carried out with c[D^4,K^8]Gal(1−16)-NH_2, a sample consisting of 1.4 mM peptide in an SDS stock solution containing 200 mM SDS in 50 mM sodium phosphate buffer (pH 6.2) was prepared. This sample was then diluted with the same SDS stock solution until the measured sample absorption at 275 nm was 0.114. A second sample of L-Trp in the same SDS stock solution was prepared with an absorption reading of 0.175 at 275 nm. For reference purposes, a third sample of L-Trp in water was made. The absorption reading for this sample at 275 nm was 0.12. Absorption spectra were recorded on a scanning UV−visible absorption spectrometer using a 1 cm path length quartz cuvette cell. The concentration of Tyr or Trp within each sample was calculated using the following absorption coefficients: ϵ = 1340 and 5550 cm M^{-1} at 280 nm for Tyr and Trp, respectively.

CD Spectroscopy. CD spectra were recorded on a Jasco J710 spectropolarimeter at 25 °C. Ten scans were collected for each sample over a wavelength range of 185−270 nm, using a 0.2 nm resolution, a 1.0 nm bandwidth, a 100 nm/min scan speed, and a 0.25 s response time. A 0.01 cm path length cell was used for experiments involving sample concentrations greater than 1.0 mM, whereas a 0.05 cm path length cell was employed for CD studies carried out on the 0.75 and 0.38 mM samples. CD analyses of the 0.075 mM peptide samples required a CD cell with a 0.1 cm path length. The collected spectra were improved through background subtraction and smoothing and then converted to units of molar ellipticity per residue (deg cm^2 $dmol^{-1}$).

NMR Spectroscopy. All NMR spectra were acquired on a Bruker DMX-600 spectrometer at 30 °C. ^1H chemical shifts were assigned using standard procedures. Two-dimensional TOCSY and NOESY experiments were carried out in the phase sensitive mode using the States−TPPI method. Acquisition of a two-dimensional data set involved sampling 512 t_1 increments with 2K data points over a 6000 Hz spectral width. Phase-shifted sine-squared window functions were applied along both dimensions, and zero filling to 2048 points was performed in the F_1 dimension prior to Fourier transformation. Mixing times employed for the TOCSY experiments were 30 and 65 ms, and NOESY spectra were acquired using mixing times of 50, 100, and 200 ms. Gradient water suppression was achieved by using the WATERGATE technique. Chemical shifts were referenced indirectly to 3,3,3-trimethylsilylpropionate.

Fluorescence Measurements. Fluorescence excitation and emission spectra were recorded on a Spex-Fluorolog 2 spectrofluorimeter. The fluorescence emission was collected from 300 to 700 nm in 1 nm increments. Emission spectra were obtained for each sample at both 275 and 295 nm excitation wavelengths. Corrections were made for the wavelength-dependent bias of the optical and detection systems, and measurements were taken using a 1 cm path length quartz cuvette cell. The quantum yield of L-Trp in a 200 mM SDS solution was first determined to be 0.07 by taking L-Trp in water (0.14) as a reference. The quantum yield of c[D^4,K^8]Gal(1−16)-NH_2 was then calculated using L-Trp in the micelle solution as a reference.

Approximating the Distance between the Tyr and Trp Aromatic Rings Using FRET Efficiencies. The efficiency of energy transfer (E) from the donor (Tyr) to the acceptor (Trp) in c[D^4,K^8]Gal(1−16)-NH_2 may be recovered from the acceptor fluorescence enhancement according to (*29*)

$$E = \left(\frac{I_{\mathrm{Trp275}}}{I_{295}} - f_{\mathrm{Trp275}}\right)/f_{\mathrm{Tyr275}} \qquad (1)$$

where I_{295} is the measured quantum yield with excitation at 295 nm, f_{Trp275} and f_{Tyr275} are the fractional absorptions of Trp and Tyr, respectively, and

$$f_{\mathrm{Trp275}} = I_{275}\left(\frac{S_{\mathrm{Trp275}}}{S_{275}}\right) \qquad (2)$$

In eq 2, I_{275} is the measured quantum yield for c[D^4,K^8]Gal-(1−16)-NH_2 with excitation at 275 nm and S_{275} is the area under the emission curve obtained for the same peptide with excitation at 275 nm. S_{Trp275} is the area under the curve acquired for the peptide with excitation at 295 nm and normalized at 380 nm to the emission curve resulting from excitation at 275 nm.

Once the transfer efficiency (E) is known, the interchromophore distance (R) between Trp^2 and Tyr^9 is calculated according to

$$R = R_o\left[\left(\frac{1}{E}\right) - 1\right]^{1/6} \qquad (3)$$

where R_o is the Förster critical distance.

The Förster critical distance R_o is calculated using the general equation (*29*)

$$R_o^6 = (8.79 \times 10^{-25})\langle\kappa^2\rangle\eta^{-4}I_D J_{AD} \quad (4)$$

where η is the refractive index, J_{AD} is the overlap integral ($J_{AD} = 4.8 \times 10^{-16}$ M^{-1} cm^{-6}), and I_D is the quantum yield of the donor (tyrosine) in the absence of acceptor. A value for I_D is obtained using the equation $I_D = I_{DA}/(1 - E)$, where

$$I_{DA} = (1 - S_{Trp275}/S_{275})(I_{275}/f_{Tyr275}) \quad (5)$$

Structure Calculations. Cross-peak intensities in the 100 ms NOESY spectrum acquired for c[D^4,K^8]Gal(1−16)-NH$_2$ were classified as weak, medium, or strong corresponding to interproton upper bound distance constraints of 5.0, 3.5, and 2.5 Å, respectively. Lower distance bounds were set to 1.8 Å in all cases.

A random starting structure for c[D^4,K^8]Gal(1−16)-NH$_2$ was generated according to the protocol of Nilges et al. (*30*, *31*). This structure was then subjected to random simulated annealing (SA) and SA structure refinement using the program X-PLOR 9.80 (MSI version) under the influence of the geometric force field, parallhdg.pr. NOE distance restraints and αH chemical shift constraints were incorporated with a square-well potential during the structure refinement protocol. A total of 100 structures were generated, and these were compared using pairwise and average rmsd values for the C$^\alpha$, C, and N atoms.

RESULTS

Analogues of Galanin(1−16) with Single Alanine Substitutions. Residues within the active galanin(1−16) peptide were systematically substituted with alanine and the resultant peptides tested for their biological activities. The synthesized galanin analogues together with their biological data are shown in Table 2. The most pronounced decrease in the level of galanin receptor binding occurred when Trp^2 was substituted with alanine. A significant loss of receptor binding was also observed when Tyr^9 was substituted for alanine in the case of GalR2 and to a lesser extent in the case of GalR1.

Optimal Cyclization Site in Galanin(1−16)-NH$_2$. Several cyclic lactam analogues of galanin(1−16)-NH$_2$ were synthesized and tested for their binding affinities for the GalR1 and GalR2 receptors. The goal of this exercise was to test whether galanin(1−16)-NH$_2$ could be conformationally constrained and still retain its biological activity. A summary of receptor binding affinities and agonist potencies measured for the cyclic peptides is presented in Table 3. According to the data presented in Table 3, c[D^4,K^8]Gal(1−16)-NH$_2$ and c[D^4,K^8]Gal(1−12)-NH$_2$ are the only cyclic analogues which bind with high affinity to both the GalR1 and GalR2 receptors. Compounds c[D^4,K^8]Gal(2−16)-NH$_2$ and c[D^4,K^8]-Gal(2−12)-NH$_2$ bound with reasonable affinity to the GalR2 receptor but with poor affinity to the GalR1 receptor, whereas the remaining analogues in Table 3 did not bind well to either receptor. None of the cyclic analogues tested were able to induce GalR1 receptor activation with a potency equivalent to that of galanin(1−16)-NH$_2$. However, GalR2 receptor agonist activity comparable to that of galanin(1−16)-NH$_2$ was observed for cyclic analogues c[D^4,K^8]Gal(1−16)-NH$_2$, c[D^4,K^8]Gal(1−12)-NH$_2$, c[D^4,K^8]Gal(2−16)-NH$_2$, and c[D^4,K^8]Gal(2−12)-NH$_2$ in Table 3. All compounds in Table 3 exhibited the same maximal effect as galanin in the assays used and are therefore full agonists.

Table 2: Alanine Scan of Galanin(1−16)

	binding		activation	
	IC$_{50}$ (nM)		EC$_{50}$ (nM)	
peptide	hGalR1	rGalR2	hGalR1	rGalR2
Gal(1−16)-NH$_2$	0.46	4.45	51	
[Ala^1]Gal(1−16)	1.54	11.0	558	
[Ala^2]Gal(1−16)	>10000	>10000		
[Ala^3]Gal(1−16)	11.7	292	7470	
[Ala^4]Gal(1−16)	1.26	8.99	969	
[Ala^5]Gal(1−16)	3.23	543	7000	335
[Ala^6]Gal(1−16)	1.02	14.4	423	
[Ala^8]Gal(1−16)	4.24	4.8	5940	
[Ala^9]Gal(1−16)	39.9	4860		3620
[Ala^{10}]Gal(1−16)	28.6	1570		799
[Ala^{11}]Gal(1−16)	4.71	431	7790	
[Ala^{12}]Gal(1−16)	3.38	53.8	4370	
[Ala^{13}]Gal(1−16)	0.40	5.13	109	
[Ala^{14}]Gal(1−16)	0.41	3.61	104	
[Ala^{16}]Gal(1−16)	0.55	4.94	210	

Table 3: Receptor Affinities and Agonist Potencies of Galanin Analogues

	binding		activation	
	IC$_{50}$ (nM)		EC$_{50}$ (nM)	
peptide	hGalR1	rGalR2	hGalR1	rGalR2
Gal(1−16)-NH$_2$	0.174	1.39	14.5	8.80
c[D^3,K^7]Gal(1−16)-NH$_2$	215	347		1510
c[D^4,K^8]Gal(1−16)-NH$_2$	0.601	1.75	1690	9.97
c[D^5,K^9]Gal(1−16)-NH$_2$	1470	>10000		
c[D^6,K^{10}]Gal(1−16)-NH$_2$	1610	1460		
c[D^4,Orn^8]Gal(1−16)-NH$_2$	91.6	300	>10000	857
c[D^4,K^8]Gal(2−16)-NH$_2$	130	4.65		18.8
c[D^4,K^8]Gal(1−12)-NH$_2$	2.06	7.16	3120	14.3
c[D^4,K^8]Gal(2−12)-NH$_2$	521	29.2	nt	25.7
c[D^4,K^7]Gal(1−16)-NH$_2$	68.7	517	>10000	nt

CD Spectroscopy. The secondary conformational features adopted by c[D^4,K^8]Gal(1−16)-NH$_2$, c[D^4,K^8]Gal(2−16)-NH$_2$, c[D^4,K^8]Gal(1−12)-NH$_2$, and c[D^4,K^8]Gal(2−12)-NH$_2$ upon interaction with SDS micelles were investigated by CD spectroscopy. To ensure that aggregation was not occurring at a peptide concentration of 1.5 mM, CD spectra were acquired for these cyclic galanin analogues using sample concentrations of 1.5, 0.75, 0.38, and 0.075 mM. The appearance of the CD spectra acquired for c[D^4,K^8]Gal(1−16)-NH$_2$, c[D^4,K^8]Gal(1−12)-NH$_2$, and c[D^4,K^8]Gal(2−12)-NH$_2$ remained constant over the entire concentration range, whereas peptide self-association was evident for c[D^4,K^8]-Gal(2−16)-NH$_2$ at concentrations above 0.75 mM. CD studies were therefore carried out on this peptide at 0.75 mM.

The shape of the CD curve obtained for c[D^4,K^8]Gal(1−16)-NH$_2$ is characteristic of a peptide with partial α helical secondary structure (Figure 1). Double minima are observed at 208 and 222 nm, and a positive band is present in the spectrum at 190 nm. A similar CD spectral profile is also observed for c[D^4,K^8]Gal(1−12)-NH$_2$. However, the negative ellipticity at 222 nm is more pronounced in this case. In comparison to that of c[D^4,K^8]Gal(1−16)-NH$_2$, the CD spectra acquired for both c[D^4,K^8]Gal(2−16)-NH$_2$ and c[D^4,K^8]Gal(2−12)-NH$_2$ exhibit a much reduced negative ellipticity at 222 nm, a decrease in intensity for the positive band at 190 nm, and a shift in the absorption maximum from 208 to 205 nm (Figure 1). These spectral changes indicate that a significant reduction in the level of α helical secondary

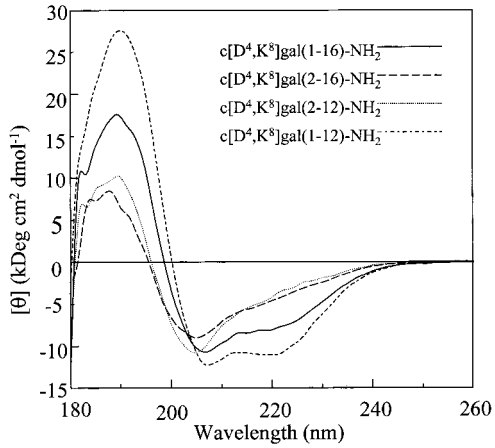

FIGURE 1: Circular dichroism spectra of c[D^4,K^8]Gal(1−16)-NH_2 and its truncated analogues in the presence of SDS micelles at 22 °C. The character θ symbolizes mean residue ellipticity.

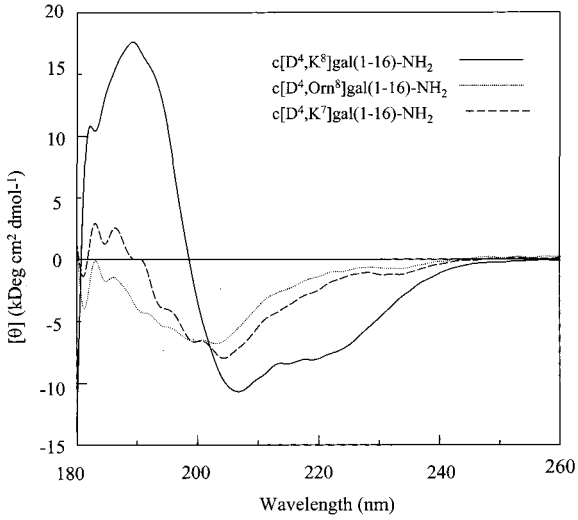

FIGURE 2: Circular dichroism spectra of cyclic galanin(1−16)-NH_2 analogues in an aqueous SDS micelle solution at 22 °C.

structure is accompanied by removal of the N-terminal glycine residue in compounds c[D^4,K^8]Gal(1−16)-NH_2 and c[D^4,K^8]Gal(1−12)-NH_2.

Modification of the residue side chain at position 8 and relocation of the lactam bridge in c[D^4,K^8]Gal(1−16)-NH_2 resulted in two cyclic galanin analogues, c[D^4,Orn^8]Gal(1−16)-NH_2 and c[D^4,K^7]Gal(1−16)-NH_2, respectively, with a reduced ring structure size. Interestingly, there was no evidence of secondary structure observed for either compound (Figure 2).

The percentage of α helicity within the conformational ensemble for each galanin analogue was calculated from the associated negative ellipticities at 222 nm (*32*). In the membrane mimetic environment, c[D^4,K^8]Gal(1−12)-NH_2 is 28% helical whereas c[D^4,K^8]Gal(1−16)-NH_2 is only 18% helical. The amount of helicity calculated for the N-terminally truncated peptides was 6 and 4% for c[D^4,K^8]Gal(2−16)-NH_2 and c[D^4,K^8]Gal(2−12)-NH_2, respectively. Galanin analogues c[D^4,K^7]Gal(1−16)-NH_2 and c[D^4,Orn^8]Gal(1−16)-NH_2 evidently do not possess any conformational order in the micelle solution (Figure 2) and were therefore excluded from this analysis.

NMR Spectroscopy. Proton chemical shift assignments for compounds c[D^4,K^8]Gal(1−16)-NH_2, c[D^4,K^8]Gal(2−16)-NH_2, c[D^4,K^8]Gal(1−12)-NH_2, and c[D^4,K^8]Gal(2−12)-NH_2 were unambiguously identified from cross-peaks in the TOCSY and NOESY spectra acquired for each peptide.

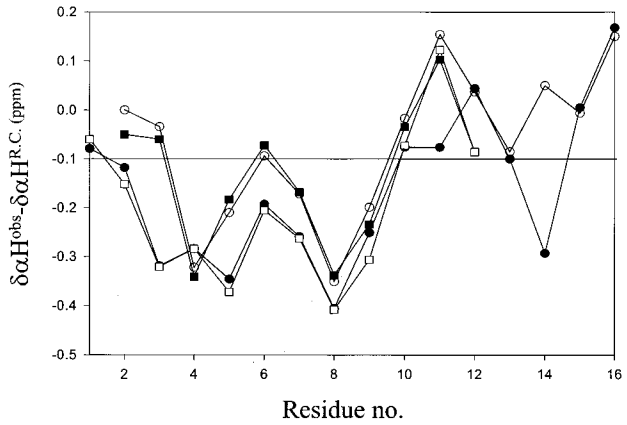

FIGURE 3: Deviation of the αH chemical shifts from random coil values ($\delta\alpha H^{obs} - \delta\alpha H^{RC}$) measured for c[D^4,K^8]Gal(1−16)-NH_2 analogues: (□) c[D^4,K^8]Gal(1−12)-NH_2, (■) c[D^4,K^8]Gal(2−12)-NH_2, (○) c[D^4,K^8]Gal(2−16)-NH_2, and (●) c[D^4,K^8]Gal(1−16)-NH_2.

The αH chemical shift in a peptide or protein provides a sensitive measure of its level of local secondary structure. In particular, a density of four or more αH chemical shifts ($\delta\alpha H^{obs}$) displaced more than 0.1 ppm upfield from random coil values ($\delta\alpha H^{RC}$) indicates a region of α helical structure (*33*). In the case of c[D^4,K^8]Gal(1−16)-NH_2 and c[D^4,K^8]-Gal(1−12)-NH_2, the values of the calculated chemical shift differences, $\delta\alpha H^{obs} - \delta\alpha H^{RC}$, were consistently more negative than −0.1 ppm for residues Trp^2−Leu^9 (Figure 3). This result suggests that a two-turn helix occupies the N-terminus of both Gly^1-containing analogues. The nearly identical αH chemical shift values obtained for these two peptides also suggest that their backbone conformations are similar. A loss of helical secondary structure resulting from removal of the N-terminal glycine is supported by the general decrease in αH resonance displacements from random coil values in the region of Trp^2−Tyr^9 observed for c[D^4,K^8]Gal-(2−16)-NH_2 and for c[D^4,K^8]Gal(2−12)-NH_2 (Figure 3). Also evident in Figure 3 is a close correlation between the αH chemical shifts measured for compounds c[D^4,K^8]Gal-(2−16)-NH_2 and c[D^4,K^8]Gal(2−12)-NH_2 which may be attributed to similarities in their backbone conformations.

NOESY spectra were acquired for compounds c[D^4,K^8]-Gal(1−16)-NH_2, c[D^4,K^8]Gal(1−12)-NH_2, c[D^4,K^8]Gal(2−16)-NH_2, and c[D^4,K^8]Gal(2−12)-NH_2 using three different mixing times. Appreciable differences in the number of NOEs and their associated intensities were not observed among the spectra acquired for each compound. Spin diffusion was therefore not a factor contributing to the NOE signal intensities. A summary of the NOEs for the four cyclic analogues is shown in Figure 4. According to the NOE data shown in Figure 4, c[D^4,K^8]Gal(1−16)-NH_2 and c[D^4,K^8]-Gal(1−12)-NH_2 are the only analogues containing a significant amount of α helical secondary structure. Noteworthy is the extended stretch of medium-range $d_{\alpha\beta}(i,i+3)$ NOEs observed in the region of Trp^2−Tyr^9 for both peptides. This type of NOE pattern is used to identify a sequence of residues adopting α helical structure (*34*). A series of $d_{\alpha N}(i,i+1)$ NOEs with intensities weaker than those of their $d_{NN}(i,i+1)$ counterparts was observed for both c[D^4,K^8]Gal(1−16)-NH_2

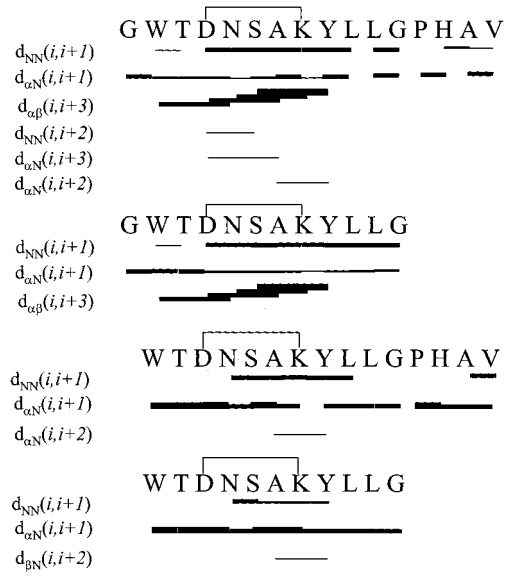

FIGURE 4: Summary of the observed NOE contacts used to determine secondary conformational features in c[D^4,K^8]Gal(1−16)-NH_2 analogues. An NOE connectivity is indicted by a bar joining the two residues that are involved. The intensity of an NOE is proportional to the height of its representative bar.

and c[D^4,K^8]Gal(1−12)-NH_2. These data are also consistent with the presence of an N-terminal helical conformation. The appearance of a weak $d_{NN}(i,i+2)$ NOE between Asp^4 and Ser^6 and a $d_{\alpha N}(i,i+3)$ NOE connecting residues Asp^4 and Ala^7 in the NOESY spectrum obtained for c[D^4,K^8]Gal(1−16)-NH_2 provides further support for the presence of a helix in this compound.

Other than a series of weak to medium-range $d_{NN}(i,i+1)$ NOEs observed in the region of Asn^5−Leu^{10} in the case of c[D^4,K^8]Gal(2−16)-NH_2 or Asn^5−Tyr^9 in the case of c[D^4,K^8]-Gal(2−12)-NH_2 (Figure 4), there were no NOEs found which support the presence of a helical conformation in either analogue. However, NOEs between residues Ala^7 and Tyr^9 (Figure 4) were obtained for both peptides, suggesting that their conformational ensembles are populated by nascent helical structures (*35*).

Fluorescence Studies. The emission maximum wavelength observed for c[D^4,K^8]Gal(1−16)-NH_2 following excitation at 275 nm was 334 nm, a value which is considerably blue shifted from that observed for L-Trp in purely aqueous solution (352 nm) and L-Trp in 200 mM SDS (350 nm; Figure 5). The most probable cause of this blue shift is insertion of the Trp^2 indole ring into the hydrophobic interior of the micelle.

Calculation of the average interchromophore distance between the Trp^2 and Tyr^9 aromatic rings in c[D^4,K^8]Gal-(1−16)-NH_2 was carried out using eqs 1−5. Measured values for the quantum yields were 0.0394 and 0.0399 for I_{Trp275} and I_{295}, respectively, and fractional absorptions were 0.81 and 0.19 for Trp and Tyr, respectively. The energy transfer efficiency (E) was determined to be 0.9 from these data. The Förster critical distance (R_o) was calculated to be 15 Å using values of 1.3, $^2/_3$, and 0.18 for the refractive index, the $\langle\kappa^2\rangle$ parameter, and I_D, respectively. This value for R_o resulted in a Tyr−Trp interaromatic ring spacing of 10.8 ± 3 Å.

The experimentally determined interchromophore separation of 10.8 ± 3 Å obtained here for c[D^4,K^8]Gal(1−16)-NH_2 is close to that previously reported for galanin(1−15)-NH_2 in water (d = 10.5 Å) (*36*). This distance is also in good agreement with the 9 Å interchromophore spacing observed in a helical galanin(1−15)-NH_2 structure generated from Monte Carlo simulations of the linear peptide (*36*). The ±3 Å error associated with the measured FRET distance is in accordance with uncertainties in the rigidity of the cyclic peptide and hence the value of $\langle\kappa^2\rangle$ which could possibly take on values between 0.15 and 2.5 (*29*).

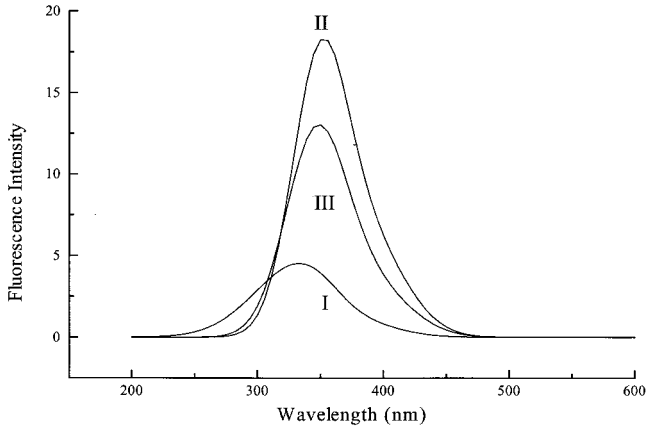

FIGURE 5: Fluorescence emission spectra of (I) c[D^4,K^8]Gal(1−16)-NH_2 in the presence of SDS micelles, (II) L-Trp in aqueous buffer, and (III) L-Trp in an SDS micelle solution. The excitation wavelength (λ_{ex} = 275 nm) was selected for excitation of the Trp indole ring.

A molecular model representing the fully extended conformation of c[D^4,K^8]Gal(1−16)-NH_2 was manually constructed. The distance measured between the Trp^2 and Tyr^9 aromatic rings in this model was 28 Å. The 10.8 ± 3 Å distance separating the two aromatic rings derived from the FRET analysis of c[D^4,K^8]Gal(1−16)-NH_2 is therefore more consistent with a folded helical conformation in the N-terminus of the molecule.

Structure Refinement for c[D^4,K^8]Gal(1−16)-NH_2. A total of 49 interresidue NOE cross-peaks were found in the 100 ms NOESY spectrum acquired for c[D^4,K^8]Gal(1−16)-NH_2. Of these, 36 corresponded to sequential NOEs while the remaining 13 NOEs were medium-range. The NOEs were assigned as weak, medium, or strong on the basis of their measured cross-peak volumes. When the calculations were performed, only the medium-range and sequential $d_{NN}(i,i+1)$ NOE-derived distance constraints were employed. The αH chemical shifts in the proposed helical region of c[D^4,K^8]-Gal(1−16)-NH_2 (i.e., Gly^1−Leu^{10}) were also used as constraints during the computational analysis of this compound.

Within the set of 100 structures generated for c[D^4,K^8]-Gal(1−16)-NH_2, 62 were accepted on the basis of their ability to satisfy the entire set of NOE constraints and the majority of the αH chemical shift restraints. A well-defined helix starting at Asp^4 and finishing at Leu^{10} became apparent following a pairwise rmsd analysis of the 62 structures (rmsd = 0.94). This conformational property is easily visualized in Figure 6 which displays a superposition of 12 of the calculated conformations for c[D^4,K^8]Gal(1−16)-NH_2. A reverse turn centered on Pro^{13} was also observed in many of the conformations. The appearance of this latter structural motif may be attributed to the inclusion of an NOE constraint connecting the γH of Leu^{11} and the αH of Val^{16} in the calculations. The presence of a turn in the C-terminus of

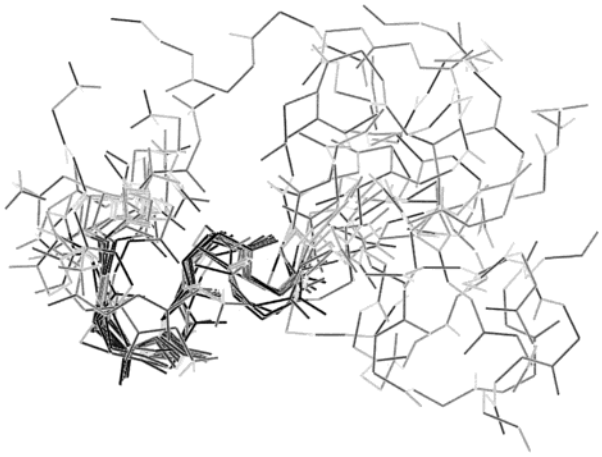

FIGURE 6: Superposition of 12 of the final MD refined structures of c[D^4,K^8]Gal(1−16)-NH_2 in the proposed helical region of Gly^1−Leu^{10}.

the cyclic galanin analogue is not unexpected since prolines are known to occupy the $i+1$ position in β-hairpin turns (*37*). However, an attempt at aligning the backbone atoms within the C-terminal segment of Gly^{12}−Val^{16} did not result in any appreciable convergence. Hence, the peptide retains some flexibility in its C-terminal region.

DISCUSSION

Replacement of amino acids at positions 4 and 8 within the linear peptide galanin(1−16)-NH_2 was a necessary first step in the synthesis of c[D^4,K^8]Gal(1−16)-NH_2 and its analogues. The importance of the two naturally occurring residues at positions 4 and 8 (Leu and Gly, respectively) within galanin(1−16) therefore needed to be evaluated. As seen in Table 2, alanine replacement at either position 4 or 8 within the linear peptide did not result in a significantly decreased level of binding to either receptor. Successful binding of analogues c[D^4,K^8]Gal(1−16)-NH_2 and c[D^4,K^8]-Gal(1−12)-NH_2 to the GalR1 receptor is thus more likely due to a conformational effect as opposed to an amino acid substitution. The most notable reductions in the level of galanin receptor binding occurred when either Trp^2 or Tyr^9 was replaced with alanine. The importance of these residues for binding is not a novel finding and has already been discussed and reported elsewhere for the GalR1 receptor (*17*, *18*). The binding data presented in Table 2 confirm the importance of these residues for GalR2 binding.

Results from the CD experiments carried out with c[D^4,K^8]-Gal(1−16)-NH_2 and c[D^4,K^8]Gal(1−12)-NH_2 indicate that these two peptides adopt helical conformations in an SDS micelle solution (Figure 1). The amount of helicity present within the conformational ensemble was, furthermore, determined to be 18 and 28% for c[D^4,K^8]Gal(1−16)-NH_2 and c[D^4,K^8]Gal(1−12)-NH_2, respectively (Figure 1). According to results obtained from the αH chemical shift analyses (Figure 3), helical conformations are assumed by residues Gly^1−Leu^{10} in both peptides. This translates to 56% of the residues within c[D^4,K^8]Gal(1−16)-NH_2 and 83% of the residues within c[D^4,K^8]Gal(1−12)-NH_2. The percentage of the conformational ensemble characterized by an N-terminal helix is, therefore, closer to 32% in the case of c[D^4,K^8]Gal-(1−16)-NH_2 and 33% in the case of c[D^4,K^8]Gal(1−12)-NH_2. These figures likely represent lower bounds, however, since the percentage of α helical structure contained in a peptide is normally underestimated by CD spectroscopy when the length of the helix does not exceed two turns (*35*). The similar values in percent helicity calculated for the two peptides implies that residues Leu^{11}−Val^{16} in c[D^4,K^8]Gal-(1−16)-NH_2 do not contribute to the helix stability.

Removal of the N-terminal glycine in peptides c[D^4,K^8]-Gal(1−16)-NH_2 and c[D^4,K^8]Gal(1−12)-NH_2 resulted in compounds with a much lower propensity to adopt a helical conformation (Figures 1, 3, and 4). It is well-known that glycine is an excellent helix-stabilizing residue when incorporated at the N-terminal position of the helix (*38*). Omission of the helix N-cap residue, Gly^1, in c[D^4,K^8]Gal(1−16)-NH_2 and c[D^4,K^8]Gal(1−12)-NH_2 would, therefore, explain the loss in the level of helical conformation observed for analogues c[D^4,K^8]Gal(2−16)-NH_2 and c[D^4,K^8]Gal(2−12)-NH_2.

The observed stretch of $d_{\alpha\beta}(i,i+3)$ NOEs between Trp^2 and Tyr^9 provided further evidence for the presence of helical conformations in compounds c[D^4,K^8]Gal(1−16)-NH_2 and c[D^4,K^8]Gal(1−12)-NH_2 (Figure 4). However, in contrast to this finding, many of the expected $d_{\alpha N}(i,i+3)$ NOEs in the proposed helical region, Gly^1−Leu^{10}, of these two peptides were not observed. Progressive fraying toward the ends of the two-turn helix would explain the absence of these NOEs as well as the low helicity estimate determined from the CD measurements (32%) (*35*). Consistent with this observation is the lack of a well-defined conformation within residues Gly^1−Thr^3 among the calculated conformations for c[D^4,K^8]-Gal(1−16)-NH_2 (Figure 6). It is, therefore, reasonable to assume that the N-terminal sequence of c[D^4,K^8]Gal(1−16)-NH_2 also adopts nonhelical conformations that are in equilibrium with the helix. However, there was no other N-terminal conformational feature present at a sufficiently high concentration to allow its detection by either NMR or CD spectroscopy.

NOEs connecting residues Ala^7 and Tyr^9 (Figure 4) were observed for the two Gly^1 deficient analogues. Such NOEs are commonly seen in spectra associated with peptide fragments adopting nascent helical structures (*35*). The presence of a weak shoulder at 222 nm in the CD spectra acquired for both analogues (Figure 1) also supports the presence of nascent helical structures. Upfield chemical shift displacements of greater than 0.1 ppm from random coil values occurred for several residues in both peptides within the sequence of Asp^4−Tyr^9 (Figure 3). On the basis of this evidence, it can be postulated that an ensemble of turn-like structures present in the region of Asp^4−Tyr^9 of c[D^4,K^8]-Gal(2−16)-NH_2 and c[D^4,K^8]Gal(2−12)-NH_2 may represent the early stage of helix folding. The N-terminal glycine in c[D^4,K^8]Gal(1−16)-NH_2 thus provides the additional stabilizing force required to trap the first 10 residues in a helical conformation.

Both c[D^4,K^8]Gal(1−16)-NH_2 and its truncated analogue c[D^4,K^8]Gal(1−12)-NH_2 adopted virtually identical helical secondary structures within the first 10 residues (Figures 1, 3, and 4) and exhibited similar binding affinities for the GalR1 receptor (Table 3). Hence, conformations in the C-terminus (residues 12−16) apparently do not contribute to GalR1 binding. The helix was furthermore the only detectable conformation in the N-terminus of both c[D^4,K^8]-

Gal(1−16)-NH_2 and c[D^4,K^8]Gal(1−12)-NH_2 and must therefore be considered as a more stable conformation for these cyclic analogues. According to the binding data and conformational profiles determined for the galanin(1−16)-NH_2 cyclic lactam analogues, neither peptide with a reduced ring structure size [c[D^4,Orn^8]Gal(1−16)-NH_2 or [D^4,K^7]Gal-(1−16)-NH_2] was able to adopt a helical conformation or bind to the GalR1 receptor. Since c[D^4,Orn^8]Gal(1−16)-NH_2 is structurally very similar to c[D^4,K^8]Gal(1−16)-NH_2 yet is conformationally undefined, it can be reasoned that the N-terminal helix in c[D^4,K^8]Gal(1−16)-NH_2 is an important determinant for GalR1 receptor binding. The observed correlation between helix formation and GalR1 receptor binding therefore allows one to hypothesize an important role for the N-terminal helix in GalR1 receptor binding.

In a recently published article by Öhman et al. (*24*), results describing the conformational properties of the full-length neuropeptide in an SDS micelle solution were presented. The molecular model of porcine galanin resulting from these studies indicated the presence of well-defined β or γ turns in three regions, including residues 1−5, 7−10, and 24−27. In contrast to this finding, the experimentally derived model for c[D^4,K^8]Gal(1−16)-NH_2 shown here contains a well-converged helix spanning residues 4−10. Secondary interactions involving residues in the C-terminus beyond Val^{16} in the full-length peptide may be responsible for these observed differences in secondary structure. However, results from ^{1}H NMR studies previously carried out on human galanin suggested that residues 3−11 may adopt an α helix in aqueous solution (*21*). Therefore, species-related inconsistencies among residues in the C-terminal sequence of galanin may result in porcine galanin exhibiting conformational behavior in solution different from that of human galanin and its analogues.

From data collected during the FRET experiments, the distance between the Trp^2 and Tyr^9 aromatic rings in c[D^4,K^8]-Gal(1−16)-NH_2 was calculated to be 10.8 ± 3 Å. This result is comparable to the 10.5 Å interchromophore spacing found for galanin(1−15)-NH_2 in water (*36*) and considerably shorter than the 28 Å interaromatic ring distance expected for the fully extended cyclic galanin analogue. Monte Carlo simulations previously carried out with galanin(1−15)-NH_2 in a hydrophobic environment resulted in low-energy N-terminal helical conformations in which the distance separating the Trp^2 and Tyr^9 aromatic rings was consistently close to 9 Å (*36*). The FRET results obtained for c[D^4,K^8]Gal-(1−16)-NH_2 in the study presented here are therefore much more characteristic of a helical conformation than an extended one.

A model describing the interaction between galanin and its GalR1 receptor was recently developed using information gained from site-directed mutagenesis studies combined with results obtained from previous conformational investigations of galanin analogues (*25*). There were four residues in the receptor identified as potential interaction sites for the critical pharmacophores in galanin. Two histidines (His^{264} and His^{267}) near the top of transmembrane domain VI were proposed to interact with Trp^2 of galanin, while Gly^1 of the neuropeptide was suggested to interact with Phe^{115} of the receptor. The Tyr^9 residue of galanin was also found to make contact with Phe^{282} in transmembrane domain VII of the GalR1 receptor. When this study was carried out, galanin was docked onto its receptor while assuming a helical conformation. Clearly, then a helical conformation in the N-terminus of galanin provides a good geometric arrangement of its critical residues for subsequent interaction with the proposed receptor binding site. On the basis of this interaction model and the results obtained here, it can be postulated that the Gly^1 residue of galanin contributes to ligand binding to the GalR1 receptor by stabilizing an α helix in the Gly^1−Leu^{10} region of the neuropeptide. By contrast, removal of the Gly^1 residue in both c[D^4,K^8]Gal(1−16)-NH_2 and c[D^4,K^8]Gal(1−12)-NH_2 analogues as well as the full-length neuropeptide did not result in a loss of binding to the GalR2 receptor. It is, therefore, possible that selectivity for the GalR1 receptor depends on galanin being able to adopt a helical conformation, while GalR2 receptor binding does not require this conformational precursor.

Within the GalR1 receptor−ligand interaction model presented by Kask et al. (*25*), all four receptor residues suggested to be important for ligand binding reside on the top of the transmembrane domains or near the membrane surface. This implies that galanin initially binds to its receptor near the surface of the membrane. A recent NMR investigation of galanin in a micelle solution incorporating a paramagnetic probe established Trp^2 as a membrane anchoring point in the molecule (*24*). Results from fluorescence experiments carried out with c[D^4,K^8]Gal(1−16)-NH_2 in the study presented here are in agreement with this finding since the emission maximum wavelength observed for c[D^4,K^8]-Gal(1−16)-NH_2 was blue shifted from that obtained for L-Trp in the same micelle environment (Figure 5). This would be expected to occur if the ring portion of Trp is inserted into the lipid interior of the micelle. Removal of this membrane-anchoring residue through amino acid substitution may partially explain why galanin analogues lacking the Trp^2 residue are inactive.

All four peptides containing an Asp^4−Lys^8 lactam bridge (peptides **2**−**5**; Table 1) exhibited GalR2 receptor binding affinities (IC_{50} values) and agonist potencies (EC_{50} values) comparable to those of galanin(1−16)-NH_2. The conformational restriction imposed by the lactam bridge is, therefore, well tolerated at the GalR2 receptor (Table 3). Removal of the N-terminal Gly^1 residue, furthermore, did not decrease GalR2 receptor affinity. From these data, it is difficult to draw any conclusions regarding conformational features that are important for GalR2 receptor binding. However, compounds c[D^4,Orn^8]Gal(1−16)-NH_2 and c[D^4,K^7]Gal(1−16)-NH_2, which contain smaller ring structures and consequently low propensities to adopt a helix (Figure 2), exhibited low-affinity binding to the GalR2 receptor. This would suggest that an N-terminal helix may also be important for the interaction of compounds c[D^4,K^8]Gal(2−16)-NH_2 and c[D^4,K^8]Gal(2−12)-NH_2 with the GalR2 receptor. In this case, a helical conformation in the Gly^1 deficient ligands would be stabilized through a receptor interaction.

In conclusion, results from structure−activity and spectroscopic investigations of cyclic galanin analogues presented here emphasize the importance of both the ring structure size and an N-terminal glycine residue for stabilizing a helical conformation in peptides c[D^4,K^8]Gal(1−16)-NH_2 and c[D^4,K^8]-Gal(1−12)-NH_2. It may be argued that this conformational feature contributes to GalR1 receptor binding since a good correlation between the extent of high-affinity binding to the

GalR1 receptor and the ability of peptides **2**−**7** (Table 1) to assume an N-terminal helix was found. However, although the GalR1 receptor affinities exhibited by compounds c[D^4,K^8]Gal(1−16)-NH_2 and c[D^4,K^8]Gal(1−12)-NH_2 were comparable to that determined for galanin(1−16)-NH_2, their agonist potencies were lower (Table 3). The helical conformation in these cyclic galanin analogues should, therefore, be considered important for GalR1 receptor binding but not necessarily for GalR1 receptor activation. It is possible that cyclic galanin analogues c[D^4,K^8]Gal(1−16)-NH_2 and c[D^4,K^8]-Gal(1−12)-NH_2 initially bind near the surface of the GalR1 receptor in a helical conformation but are subsequently unable to undergo the necessary conformational rearrangement that is appropriate for eliciting high agonist potency.

ACKNOWLEDGMENT

We thank Stephane Lanthier (Biotechnology Research Institute CNRC, Montreal, PQ) for optimizing conditions for suspension growth of HEK293S-rGR2 and Bowes melanoma cells. We also thank Dr. Michel Belletete from the University of Montreal (Montreal, PQ) for valuable assistance with interpretation and acquisition of fluorescence spectra.

REFERENCES

1. Tatemoto, K., Rökaeus, A., Jörnvall, H., McDonald, T. J., and Mutt, V. (1983) *FEBS Lett. 164*, 124−128.
2. Bersani, M., Johnsen, A. H., Højrup, P., Dunning, B. E., Andreasen, J. J., and Holst, J. J. (1991) *FEBS Lett. 283*, 189−194.
3. Rökaeus, A. (1987) *Trends Neurosci. 10*, 158−164.
4. Nörberg, A., Sillard, R., Carlquist, M., Jörnvall, H., and Mutt, V. (1991) *FEBS Lett. 288*, 151−153.
5. Tatemoto, T. J., Dupre, J., Tatemoto, K., Greenberg, G. R., Radziuk, J., and Mutt, V. (1985) *Diabetes 34*, 192−196.
6. Amiranoff, B., Lorinet, A.-M., Lagny-Pourmir, I., and Laburthe, M. (1988) *Eur. J. Biochem. 177*, 147−152.
7. Hulting, A.-L., Meister, B., Carlsson, L., Hilding, A., and Isaksson, O. (1991) *Acta Endocrinol. 125*, 518−525.
8. Fisone, G., Wu, C. F., Consolo, S., Nordström, Ö., Brynne, N., Bartfai, T., Melander, T., and Hökfelt, T. (1987) *Proc. Natl. Acad. Sci. U.S.A. 84*, 7339−7343.
9. Kyrkouli, S. E., Stanley, B. G., Hutchinson, R., Seirafi, R. D., and Leibowitz, S. F. (1990) *Brain Res. 521*, 185−191.
10. Wiesenfeld-Hallin, Z., Xu, X.-J., Langel, Ü., Bedecs, K., Hökfelt, T., and Bartfai, T. (1992) *Proc. Natl. Acad. Sci. U.S.A. 89*, 3334−3337.
11. Habert-Ortoli, E., Amiranoff, B., Loquet, I., Laburthe, M., and Mayaux, J.-F. (1994) *Proc. Natl. Acad. Sci. U.S.A. 91*, 9780−9783.
12. Parker, E. M., Izzarelli, D. G., Nowak, H. P., Mahle, C. D., Iben, L. G., Wang, J., and Goldstein, M. E. (1995) *Mol. Brain Res. 34*, 179−189.
13. Wang, S., Hashemi, T., He, C., Strader, C., and Bayne, M. (1997) *Mol. Pharmacol. 52*, 337−343.
14. Wang, S., He, C., Hashemi, T., and Bayne, M. (1997) *J. Biol. Chem. 272*, 31949−31952.
15. Wang, S., He, C., Maguire, M., Clemmons, A., Burrier, R., Guzzi, M., Strader, C., Parker, E., and Bayne, M. (1997) *FEBS Lett. 411*, 225−230.
16. Howard, A. D., Tan, C., Shiao, L.-L., Palyha, O. C., McKee, K. K., Weiger, D. H., Feighner, S. D., Cascieri, M. A., Smith, R. G., Van Der Ploeg, L. H. T., and Sullivan, K. A. (1997) *FEBS Lett. 405*, 285−290.
17. Land, T., Langel, Ü., Löw, M., Berthold, M., Undén, A., and Bartfai, T. (1991) *Int. J. Pept. Protein Res. 38*, 267−272.
18. Amiranoff, B., Lorinet, A.-M., Yanaihara, N., and Laburthe, M. (1989) *Eur. J. Pharmacol. 163*, 205−207.
19. Fisone, G., Berthold, M., Bedecs, K., Unden, A., Bartfai, T., Bertorelli, R., Consolo, S., Crawley, J., Martin, B., Nilsson, S., et al. (1989) *Proc. Natl. Acad. Sci. U.S.A. 86*, 9588−9591.
20. Rigler, R., Wennerberg, A., Cooke, R. M., Elofsson, A., Nilsson, L., Vogel, H., Holley, L. H., Carlquist, M., Langel, U., Bartfai, T., and Campbell, I. D. (1991) in *Galanin. A New Multifunctional Peptide in the Neuro-Endocrine System* (Hökfelt, T., Bartfai, T., Jacobowitz, D., and Ottoson, D., Eds.) pp 17−25, Macmillan, London.
21. Morris, M. B., Ralston, G. B., Biden, T. J., Browne, C. L., King, G. F., and Iismaa, T. P. (1995) *Biochemistry 34*, 4538−4545.
22. Wennerberg, A. B. A., Cooke, R. M., Carlquist, M., Rigler, R., and Campbell, I. D. (1990) *Biochem. Biophys. Res. Commun. 166*, 1102−1109.
23. Öhman, A., Davydov, R., Backlund, B. M., Langel, U., and Gräslund, A. (1996) *Biophys. Chem. 59*, 185−192.
24. Öhman, A., Lycksell, P. O., Juréus, A., Langel, U., Bartfai, T., and Gräslund, A. (1998) *Biochemistry 37*, 9169−9178.
25. Kask, K., Berthold, M., Kahl, U., Nordvall, G., and Bartfai, T. (1996) *EMBO J. 15*, 236−244.
26. Öhman, A., Lycksell, P. O., Andell, S., Langel, U., Bartfai, T., and Gräslund, A. (1995) *Biochim. Biophys. Acta 1236*, 259−265.
27. Lorenzen, A., Fuss, M., Vogt, H., and Schwabe, U. (1993) *Mol. Pharmacol. 44* (1), 115−123.
28. Traynor, J. R., and Nahorski, S. R. (1995) *Mol. Pharmacol. 47* (4), 848−854.
29. Mély, Y., Jullian, N., Morellet, N., DeRocquigny, H., Dong, C. Z., Piémont, E., Roques, B. P., and Gérard, D. (1994) *Biochemistry 33*, 12085−12091.
30. Nilges, M., Clore, G. M., and Gronenborn, A. M. (1988) *FEBS Lett. 239*, 129−136.
31. Nilges, M., Clore, G. M., and Gronenborn, A. M. (1988) *FEBS Lett. 229*, 317−324.
32. Chen, Y. H., Yang, J. T., and Martinez, H. M. (1972) *Biochemistry 11*, 4120−4131.
33. Wishart, D. S., Sykes, B. D., and Richards, F. M. (1992) *Biochemistry 31*, 1647−1651.
34. Barsukov, I. L., and Lian, L.-Y. (1993) in *NMR of Macromolecules* (Roberts, G. C. K., Ed.) Oxford University Press, New York.
35. Dyson, H. J., and Wright, P. E. (1991) *Annu. Rev. Biophys. Biophys. Chem. 20*, 519−538.
36. Wiczk, W., Rekowski, P., Kupryszewski, G., Lubkowski, J., Oldziej, S., and Liwo, A. (1996) *Biophys. Chem. 58*, 303−312.
37. Muller, G., Gurrath, M., Kurz, M., and Kessler, H. (1993) *Proteins: Struct., Funct., Genet. 15*, 235−251.
38. Chakrabartty, A., Doig, A. J., and Baldwin, R. L. (1993) *Proc. Natl. Acad. Sci. U.S.A. 90*, 11332−11336.

BI991081I